

## Original Article

# Artemether attenuates renal tubular injury by targeting mitochondria in adriamycin nephropathy mice

Xinyuan Cheng<sup>1\*</sup>, Peng Zhou<sup>1\*</sup>, Wenci Weng<sup>1</sup>, Zhijian Sun<sup>1</sup>, Honghong Liu<sup>3</sup>, Yinghui Chen<sup>1</sup>, Yuchun Cai<sup>1</sup>, Xuewen Yu<sup>2</sup>, Taifen Wang<sup>1</sup>, Mumin Shao<sup>2</sup>, Wuyong Yi<sup>1</sup>, Tiegang Yi<sup>1</sup>, Huili Sun<sup>1</sup>, Pengxun Han<sup>1</sup>

Departments of <sup>1</sup>Nephrology, <sup>2</sup>Pathology, Shenzhen Traditional Chinese Medicine Hospital, The Fourth Clinical Medical College of Guangzhou University of Chinese Medicine, Shenzhen, Guangdong, China; <sup>3</sup>Department of Nephrology, Shenzhen Traditional Chinese Medicine Hospital Affiliated to Nanjing University of Chinese Medicine, Shenzhen, Guangdong, China. \*Equal contributors.

Received November 6, 2021; Accepted March 3, 2022; Epub March 15, 2022; Published March 30, 2022

**Abstract:** Chronic kidney disease (CKD) is complex and current treatment remains limited. As we know, glomerular injury plays a dominant role in kidney disease progression. However, accumulating evidence demonstrated that renal tubules, rather than being victims or bystanders, are major initiators in renal fibrosis progression. Renal tubules are rich in mitochondria and mitochondrial dysfunction may participate in renal tubular phenotypic changes and ultimately promote renal fibrosis. Previous studies have proved that artemether displayed renal protective effects, but the mechanisms remain unclear. In this experiment, we showed that artemether reduced urinary protein/creatinine ratio and attenuated renal tubular injury. Both in vivo and in vitro results indicated that artemether could restore renal tubular phenotypic alterations. Meanwhile, the unbalanced expressions of Bax and Bcl-xL in renal tubules were restored by artemether. In addition, artemether also regulated mitochondrial pyruvate metabolism, increased mitochondrial biogenesis, and improved mitochondrial function. Taken together, this study suggested that artemether could attenuate renal tubular injury by regulating mitochondrial biogenesis and function. It has great potential to be translated to the clinic as a therapeutic agent for treating kidney diseases, especially those associated with renal tubular injury.

**Keywords:** Artemether, renal tubular injury, mitochondria, adriamycin nephropathy

## Introduction

Chronic kidney disease (CKD) is complex and affects approximately 10% people globally. The etiology of CKD is heterogeneous and current treatment remains limited [1]. Therefore, better understanding of the underlying pathogenesis is urgently needed for developing effective therapies targeting CKD.

Previous investigations have suggested that glomerular injury plays a dominant role in kidney disease development and progression. However, growing numbers of studies revealed that renal tubules, rather than being victims or bystanders, are major initiators in renal fibrosis progression [2]. In the classic mouse model of adriamycin nephropathy (AN), it is generally accepted that podocyte damage was the main contributor and renal tubular injury was result-

ed from persistent proteinuria [3]. Recent studies have shown that renal tubular injury occurred during the initial phase of adriamycin injection and could trigger glomerular injury [4]. In response to external stimuli, renal tubules manifest cellular phenotypic alteration, mitochondrial dysfunction, cell cycle arrest and intracellular signaling pathways disorder [5-7].

Mitochondrial dysfunction and redox imbalance were regarded as the critical pathophysiologic mechanisms underlying the cytotoxicity of adriamycin [8-10]. At the same time, cell phenotype also changes to adapt to these pathophysiological processes. As the hub of substance and energy metabolism, mitochondria were closely related to cell morphological alterations [11]. Considering that renal tubules are rich in mitochondria and constitute major part of the kidney, we hypothesize that mitochondrial dys-

function may participate in renal tubular phenotypic changes and ultimately promote kidney fibrosis.

Artemether is an artemisinin analogue and served as anti-malaria drug. It was reported that artemisinin-based drugs displayed anti-fungal, antibacterial, anti-HIV, anticancer, and antidiabetic properties [12]. In addition, they also exhibited certain renal protection property [13-15], but the detailed mechanisms remain unclear. In this study, we explored the importance of phenotypic changes and mitochondrial function in the progression of renal tubular injury, and demonstrated that artemether may exert renal tubular protection by targeting mitochondria.

### Materials and methods

#### *Animal experiments*

Animal experiments were approved by Institutional Animal Care and Use Committee at the Guangzhou University of Chinese Medicine (Approval number: 20200331002). Male BALB/c mice (20-25 g) were obtained from Laboratory Animal Center of Southern Medical University (Guangzhou, China). Adriamycin (10.4 mg/kg, Sigma-Aldrich, St. Louis, MO, USA) was injected via tail vein to induce AN mouse model. Mice in normal control group were injected with saline solution. After two weeks, mice were divided randomly into AN group, AN+artemether (AN+Art) group, and control group. Mice in AN+Art group were fed with medicated feed containing 0.3 g/kg artemether (ConBon biotechnology, Chengdu, Sichuan, China). The normal control and AN groups were fed with standard diet. The intervention lasted for two weeks.

#### *Cell culture and treatment*

Normal rat kidney epithelial cells (NRK-52E, ATCC, Manassas, VA, USA) were cultured in the condition as previously described [15]. Cells were cultured in 24-wells plates for 24 hours to attach. Then they were treated with adriamycin (1  $\mu$ M) containing different concentrations of artemether (0, 50, 100, 150  $\mu$ M) for 24 hours.

#### *Urinary protein/creatinine and renal H<sub>2</sub>O<sub>2</sub> assay*

The total protein and creatinine in urine were measured by the Bradford method and bio-

chemical method respectively [15]. H<sub>2</sub>O<sub>2</sub> content in renal tissue homogenate was measured by the Amplex UltraRed reagent (Invitrogen, Carlsbad, CA, USA) according to the manufacturer's protocol.

#### *Pathological analysis*

At the end of the study, mice were sacrificed and the kidney tissues were collected. Paraffin-embedded kidney slices were stained with periodic acid-Schiff (PAS) to evaluate renal tubular injury. Twenty tubular areas were randomly selected in each sample and the index was scored 0 to 4 (0, <5%; 1, 5-25%; 2, 25-50%; 3, 50-75%; 4, >75%), as previously described [10].

#### *Immunohistochemistry*

Immunohistochemical staining was performed according to the previous method [10]. Briefly, kidney slices were deparaffinized and rehydrated. Subsequently, the slices were boiled in citrate buffer for antigen unmasking. After rinsing, the slices were incubated with primary antibody against vimentin (CST, Danvers, MA, USA), zonula occludens-1 (ZO-1, Invitrogen), Bax (CST), and Bcl-xL (CST) respectively overnight at 4°C. Then the slices were rinsed and incubated with secondary antibodies (MaiXin, Fuzhou, China). DAB solution was used as a chromogen and the slices were counterstained with hematoxylin.

#### *Immunoblotting analysis*

Samples of renal tissue and cell culture were homogenized and prepared in sample loading buffer (Bio-Rad). Total protein was separated by SDS-PAGE gels and transferred to PVDF membranes (Merck Millipore, Danvers, MA, USA). After blocking with 5% milk for 1 h at room temperature, the membranes were incubated overnight at 4°C with the following primary antibodies: p-E-cadherin (S838+S840), vimentin, ZO-1, cleaved PARP, Bax, Bcl-xL, PDH (pyruvate dehydrogenase), PDP1 (pyruvate dehydrogenase phosphatase 1), PDK1 (pyruvate dehydrogenase kinase 1), OPA1 (optic atrophy 1), VDAC (voltage-dependent anion channel), ERR $\alpha$  (estrogen-related receptor  $\alpha$ ), NRF1 (nuclear respiratory factor 1), HSP60 (60 kDa heat shock protein), and  $\beta$ -actin. After incubating with secondary antibodies, the membranes were imaged by the ChemiDoc Imaging System (Bio-Rad). Primary antibodies were obtained

**Table 1.** Sequences of the primers for qPCR

Gene	Primer Sequence (5'-3')
Mouse Kim-1	F: GTTAAACCAGAGATCCACACG R: TCTCATGGGGACAAAATGTAGTG
Mouse ND1	F: CTAGCAGAAACAAACCGGGC R: CCGGCTGCGTATTCTACGTT
Mouse $\beta$ -actin	F: GGACTCCTATGTGGGTGACG R: AGGTGTGGTGCCAGATCTTC

from different companies and listed below. p-E-cadherin (S838+S840): Abcam (Cambridge, UK); Vimentin, cleaved PARP, Bax, Bcl-xL, PDH, PDP1, VDAC, ERR $\alpha$ , NRF1, and HSP60: CST; PDK1: Enzo Life Science (Farmingdale, NY, USA); OPA1: BD Biosciences (Franklin Lakes, NJ, USA); ZO-1: Invitrogen;  $\beta$ -actin: Sigma Aldrich.

#### *mRNA analysis and mitochondrial DNA (mtDNA) copy number measurement*

Total RNA and genomic DNA (gDNA) in kidney tissue were extracted by RNA purification kit (Invitrogen) and gDNA purification kit (Magen, Guangzhou, China) respectively. First-strand cDNA was synthesized by using reverse transcriptase (Invitrogen) and gene specific primers (**Table 1**) were generated by Sangon Biotechnology Company (Shanghai, China). Quantitative real-time PCR (qPCR) was performed on the Applied Biosystems QuantStudio 5 platform and the amplification conditions were set as previously described [15]. The relative mRNA expression and mtDNA copy number were calculated by  $2^{-\Delta\Delta CT}$ .

#### *Statistical analysis*

For in vivo animal study, \* symbol means compare with the control group; # symbol means compare with the AN group. For in vitro cell study, \* symbol means compare with the Adriamycin: 0+Art: 0 group; # symbol means compare with the Adriamycin: 1+Art: 0 group. Data are presented as the mean  $\pm$  SD. One-way analysis of variance (ANOVA) followed by Bonferroni post hoc analysis or unpaired Student's t-test were used for data analysis using SPSS software (IBM, NY, USA).  $P < 0.05$  was considered significant.

## Results

### *Artemether reduced urinary protein/creatinine ratio and attenuated renal tubular injury*

As shown in **Figure 1A**, the ratio for urinary protein/creatinine was significantly increased in AN group and was obviously decreased by artemether therapy. The PAS staining of renal tubules and mRNA analysis of Kim-1 in kidney together demonstrated that obviously tubular injury occurred in AN group (**Figure 1B-D**). Artemether treatment significantly reduced Kim-1 mRNA level and attenuated renal tubular pathological injury (**Figure 1B-D**).

### *Artemether restored renal tubular phenotypic changes*

In order to adapt to changes of the external environment, renal tubules underwent phenotypic alterations. After exposure to adriamycin, AN group mice displayed significantly decreased p-E-cadherin and increased vimentin in renal tubules (**Figure 2A-C**). Consistent with immunoblotting results, the immunohistochemical staining also indicated that vimentin expression was obviously upregulated in AN group (**Figure 2E**). These phenotypic changes were significantly restored after artemether treatment (**Figure 2A-C** and **2E**). As the main component of tight junctions, ZO-1 in renal tubules reduced significantly in AN group (**Figure 2A** and **2D**). The immunohistochemical staining showed that the morphological distribution of ZO-1 was obviously abnormal (**Figure 2F**). Artemether therapy significantly upregulated ZO-1 expression and improved its distribution (**Figure 2A, 2D** and **2F**).

To investigate whether artemether has direct effect on cell phenotypic alterations, we performed the following cell research. NRK-52E cells were exposed to 1  $\mu$ M adriamycin and treated with different concentrations of artemether for 24 hours. Compared with control group (Adriamycin: 0+Art: 0 group), adriamycin significantly decreased ZO-1 and p-E-cadherin expression (**Figure 3A-C**). Meanwhile, significantly increased cleaved PARP was induced by adriamycin (**Figure 3A** and **3D**). The treatment of artemether dose-dependently increased

## Artemether attenuates renal tubular injury

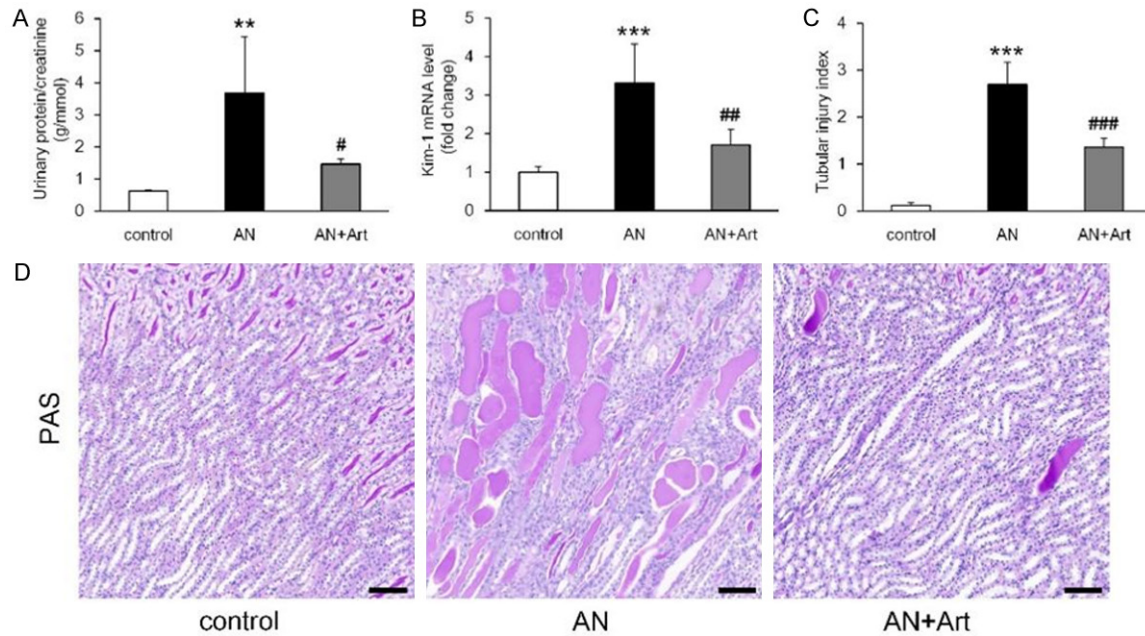


**Figure 1.** Artemether reduced urinary protein/creatinine ratio and attenuated renal tubular injury. A. Determination of the ratio for urinary protein/creatinine in various groups. B. Quantification and analysis of Kim-1 mRNA expression level in different groups. C. Evaluation of renal tubular injury in each group under PAS staining. D. Representative images of PAS staining for renal tubules (scale bar, 50  $\mu$ m). n=6 per group. \*\*P<0.01 and \*\*\*P<0.001 vs. control; #P<0.05, ##P<0.01 and ###P<0.001 vs. AN.

ZO-1 and p-E-cadherin, and decreased cleaved PARP (**Figure 3A-D**).

### *Artemether regulated mitochondria associated Bax and Bcl-xL expression*

Mitochondria damage is closely associated with cell phenotypic changes. The proportion of Bax and Bcl-xL played a key role in maintaining the morphology and function of mitochondria [16]. As shown in **Figure 4A-C**, significantly increased Bax and decreased Bcl-xL were detected in AN group. Immunohistochemical staining revealed that Bax and Bcl-xL were mainly located in renal tubules and the expression levels were consistent with the immunoblotting results (**Figure 4D and 4E**). After artemether treatment, the imbalance of Bax and Bcl-xL expression was well restored, and their pathological lesions were also obviously attenuated (**Figure 4A-E**).

### *Artemether regulated mitochondrial pyruvate metabolism*

Renal tubules are rich in mitochondria and pyruvate metabolism plays an important role in energy maintenance and mitochondrial function [17]. Pyruvate is converted to acetyl-CoA by

PDH. PDK1 phosphorylates PDH to suppress its activity, while PDP1 dephosphorylates PDH to enhance its activity [18]. Compared to control group, AN group displayed significantly decreased PDH and increased PDP1/PDK1 ratio (**Figure 5A-C**). After artemether treatment, PDH was increased slightly, but not to a significant degree (**Figure 5A and 5B**). While the increased PDP1/PDK1 ratio was reduced remarkably (**Figure 5A and 5C**).

### *Artemether increased renal tubular mitochondrial content*

OPA1 and VDAC are representative mitochondrial inner and outer mitochondrial membrane respectively [19, 20]. Compared to control group, OPA1 and VDAC both reduced significantly in AN group (**Figure 6A-C**). Meanwhile, the mtDNA copy number in AN group also decreased obviously (**Figure 6D**).  $H_2O_2$  is an important signaling molecule and its production reflects the functional status of mitochondria [21]. As shown in **Figure 6E**, the  $H_2O_2$  content in renal tissue homogenate decreased significantly in AN group. These results together indicated that mitochondrial deficiency occurred in mice after adriamycin exposure. Artemether treatment significantly raised OPA1



## Artemether attenuates renal tubular injury

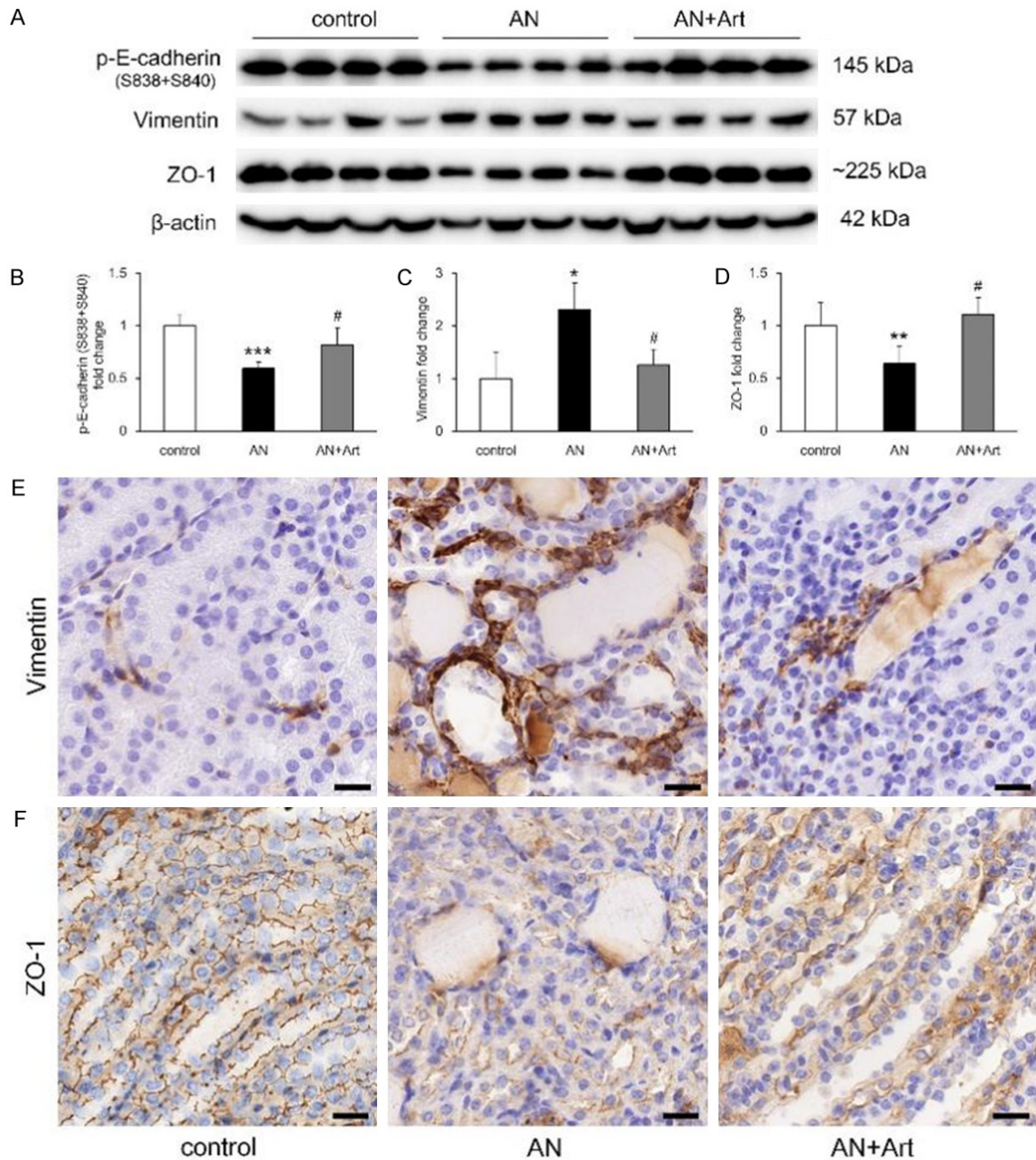


**Figure 2.** Artemether improved renal tubular phenotypic alterations. A-D. Immunoblotting images and semi-quantitative analysis of p-E-cadherin (S838+S840), vimentin, and ZO-1 in renal tissue of different groups. E, F. Representative immunohistochemical staining images of vimentin and ZO-1 in kidney. The images displayed their morphological distribution in renal tubules. Scale bar, 20  $\mu$ m. n=4 per group. \* $P$ <0.05, \*\* $P$ <0.01 and \*\*\* $P$ <0.001 vs. control; # $P$ <0.05 vs. AN.

and VDAC expression, mtDNA copy number, and  $H_2O_2$  content in kidney (Figure 6A-E).

*Artemether upregulated mitochondrial biogenesis related transcription factors*

As the related transcription factors regulating mitochondrial biogenesis and function, ERR $\alpha$ ,

NRF1, and HSP60 all reduced significantly in AN group (Figure 7A-D). The changes of these proteins well explained the mitochondrial deficiency induced by adriamycin. After artemether therapy, ERR $\alpha$  and NRF1 were raised significantly (Figure 7A-C), HSP60 was raised to some extent but not to a significant degree (Figure 7A and 7D).

## Artemether attenuates renal tubular injury

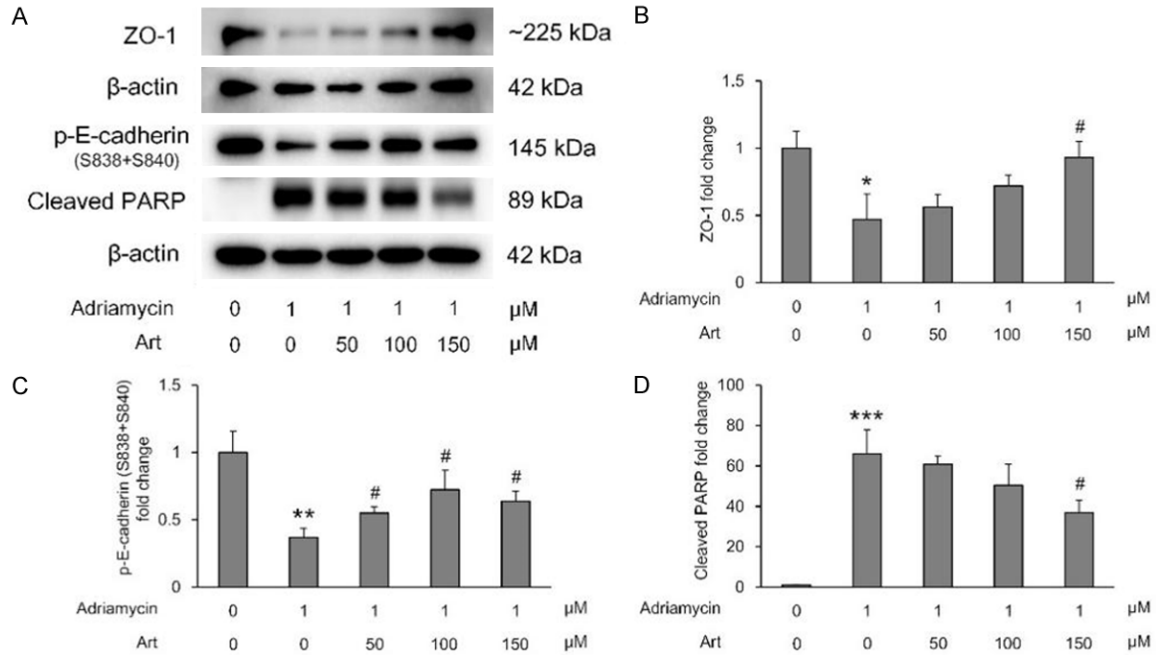


**Figure 3.** Effects of artemether on renal tubular phenotypic changes in vitro. A. Representative immunoblotting images of ZO-1, p-E-cadherin (S838+S840), and cleaved PARP after exposure to adriamycin and treated with different concentrations of artemether. B-D. Bar graphs displaying the semi-quantitative analysis of these proteins against  $\beta$ -actin.  $n=3$  per group. \* $P<0.05$ , \*\* $P<0.01$  and \*\*\* $P<0.001$  vs. Adriamycin: 0+Art: 0 group; # $P<0.05$  vs. Adriamycin: 1+Art: 0 group.

### Discussion

Accumulating evidences verified that renal tubules play a key role in kidney damage and fibrosis. Here we reported that artemether significantly attenuated renal tubular injury by targeting mitochondria in AN mice.

Urinary protein/creatinine ratio is a marker of kidney damage and Kim-1 is a representative of tubular injury [22]. In this study, artemether significantly reduced urinary protein/creatinine ratio and Kim-1 mRNA level in kidney. Consistent with the biochemical indicators, pathological lesions of renal tubules were also obviously attenuated by artemether treatment. In response to various stimuli, renal tubules lose epithelial features and gain mesenchymal characteristics [5]. Tight junction is an important factor in maintaining renal tubule function [23]. With changes of cell phenotype, the tight junction of renal tubules was also impaired which was proved by significantly reduced ZO-1. These molecular pathological alterations were obviously attenuated by artemether. Consistent with in vivo results, the in vitro study indicated that adriamycin treatment induced downregula-

tion of p-E-cadherin and ZO-1 in NRK-52E cells. Co-incubation of artemether dose-dependently upregulated their expression. Meanwhile, up-regulated cleaved PARP was also downregulated by artemether. These results suggested that cell death pathways were closely related to phenotypic alterations.

Mitochondria are essential organelle and have been implicated in multiple cellular signal pathways [24]. To explore the intracellular changes of renal tubules undergoing phenotypic remodeling, we determined the mitochondria associated proteins participating in cell death and metabolism. Bax plays a key role in mitochondria dependent apoptosis and generally expressed at a low level in cytosol, or weakly associated to mitochondria. In response to apoptotic stimuli, Bax is relocated to the outer mitochondrial membrane and participates in mitochondrial destruction process. On the contrary, Bcl-xL could retrotranslocate Bax from mitochondria to cytosol and then promote cell survive [25]. In this study, increased Bax and decreased Bcl-xL were observed in AN group. Corresponding to these lesions, mitochondria also displayed metabolic rearrangements. Py-



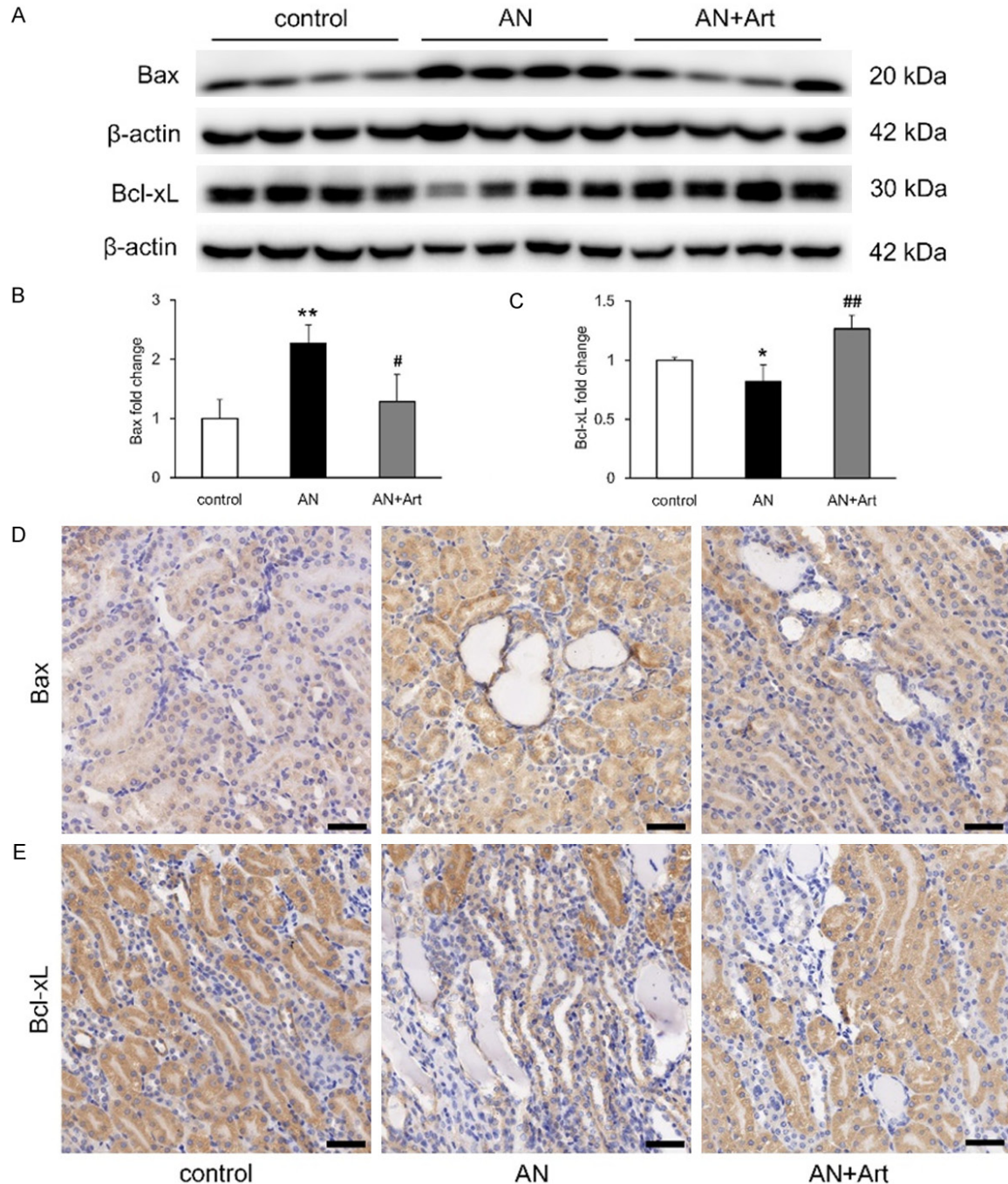


**Figure 4.** Effects of artemether on Bax and Bcl-xL expression in kidney. A. Immunoblotting bands of Bax and Bcl-xL in different groups. B, C. Bar graphs displaying the semi-quantitative analysis of Bax and Bcl-xL in each group. D, E. Immunohistochemical staining of Bax and Bcl-xL in kidney of each group. The representative images revealed that they are mainly distributed in renal tubules. Scale bar, 40  $\mu$ m. n=4 per group. \* $P$ <0.05 and \*\* $P$ <0.01 vs. control; # $P$ <0.05 and ## $P$ <0.01 vs. AN.

ruvate is metabolized in mitochondria and fuels the citric acid cycle to maintain oxidative phosphorylation. The expression of enzymes related to pyruvate metabolism including PDH, PDP1, and PDK1 were disturbed. Artemether

treatment restored the imbalance of Bax and Bcl-xL, and improved pyruvate metabolism.

The mitochondria are double membrane bound organelles. OPA1 and VDAC were localized to

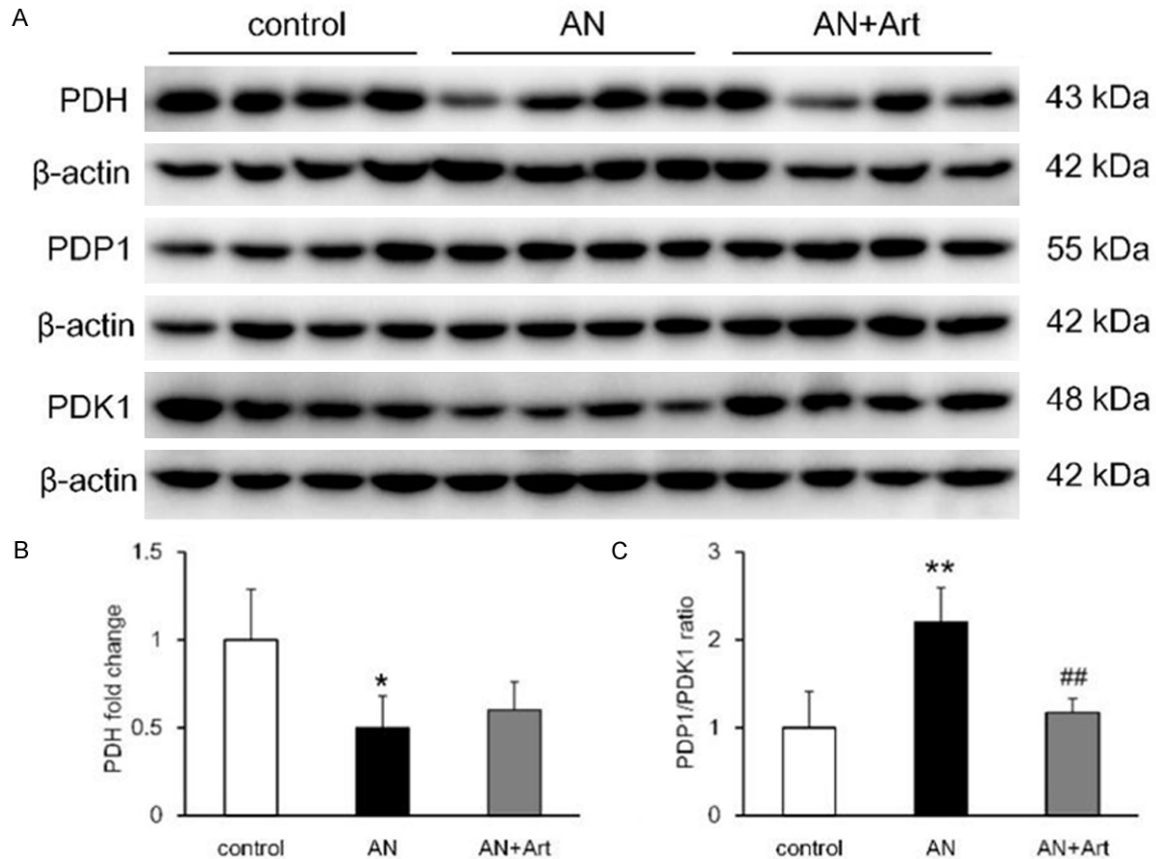


**Figure 5.** Artemether regulated mitochondrial pyruvate metabolism. A. Immunoblotting images of PDH, PDP1, and PDK1 in various groups. B, C. Bar graphs showed the fold change of PDH and PDP1/PDK1 ratio in different groups. n=4 per group. \*P<0.05 and \*\*P<0.01 vs. control; ##P<0.01 vs. AN.

the inner and outer mitochondrial membrane respectively. Consistent with the expression levels of OPA1 and VDAC in kidney, mtDNA content also reduced significantly in AN group.  $H_2O_2$  was mainly generated in mitochondria and participates in multiple signal transduction. Its production may be used as an indicator to evaluate mitochondrial content and function [26]. In AN group,  $H_2O_2$  content in renal tissue significantly reduced. These results together suggested that mitochondrial deficiency may play a critical role in renal disease progression. Considering that ERR $\alpha$ , NRF1, and HSP60 are closely related to mitochondrial biogenesis and function [27-29], we speculate that mitochondrial deletion in AN group might be associated with decreased ERR $\alpha$ , NRF1, and HSP60. It is worth mentioning that these mitochondria related alterations were obviously attenuated by artemether therapy.

In summary, this study provided some evidence that artemether could attenuate renal tubular

injury and improve cell phenotypic changes. The underlying mechanisms might be associated with its regulation on mitochondrial function and biogenesis. Taken together, our results demonstrate that artemether may be translated into clinic for treating kidney diseases, especially those associated with renal tubular injury.

#### Acknowledgements

This study was supported by grants from the National Natural Science Foundation of China (82004156), Shenzhen Science and Technology Project (JCYJ20190812183603627), and Shenzhen Fund for Guangdong Provincial High Level Clinical Key Specialties.

#### Disclosure of conflict of interest

None.

**Address correspondence to:** Pengxun Han and Huili Sun, Department of Nephrology, Shenzhen Tradi-



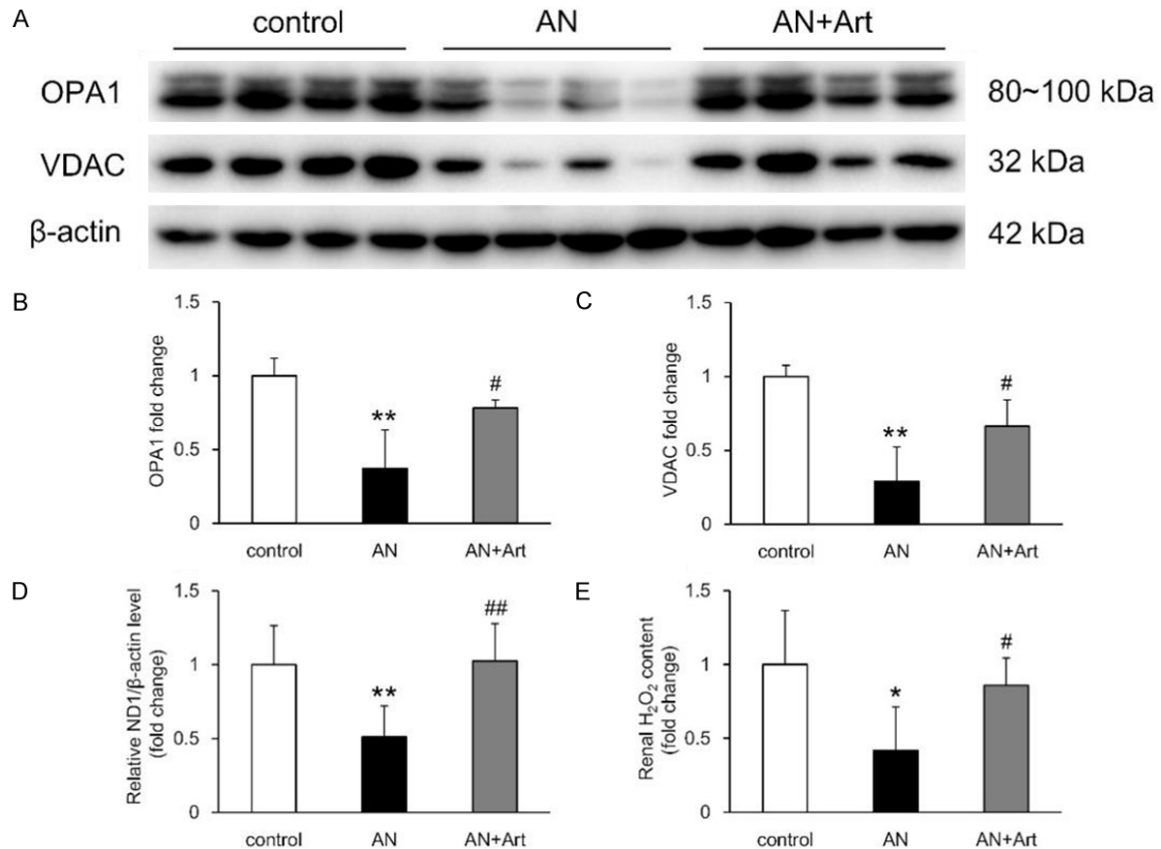


**Figure 6.** Regulating effects of artemether on renal tubular mitochondrial content. A-C. Immunoblotting bands and quantitative analysis of OPA1 and VDAC in renal tissue of various groups. n=4 per group. D. Bar graph showed the quantitative analysis of mtDNA copy number (determined by qPCR for ND1 against  $\beta$ -actin) in each group. E. Bar graph displayed the fold change of renal H<sub>2</sub>O<sub>2</sub> content in various groups. n=6 per group. \*P<0.05 and \*\*P<0.01 vs. control; #P<0.05 and ##P<0.01 vs. AN.

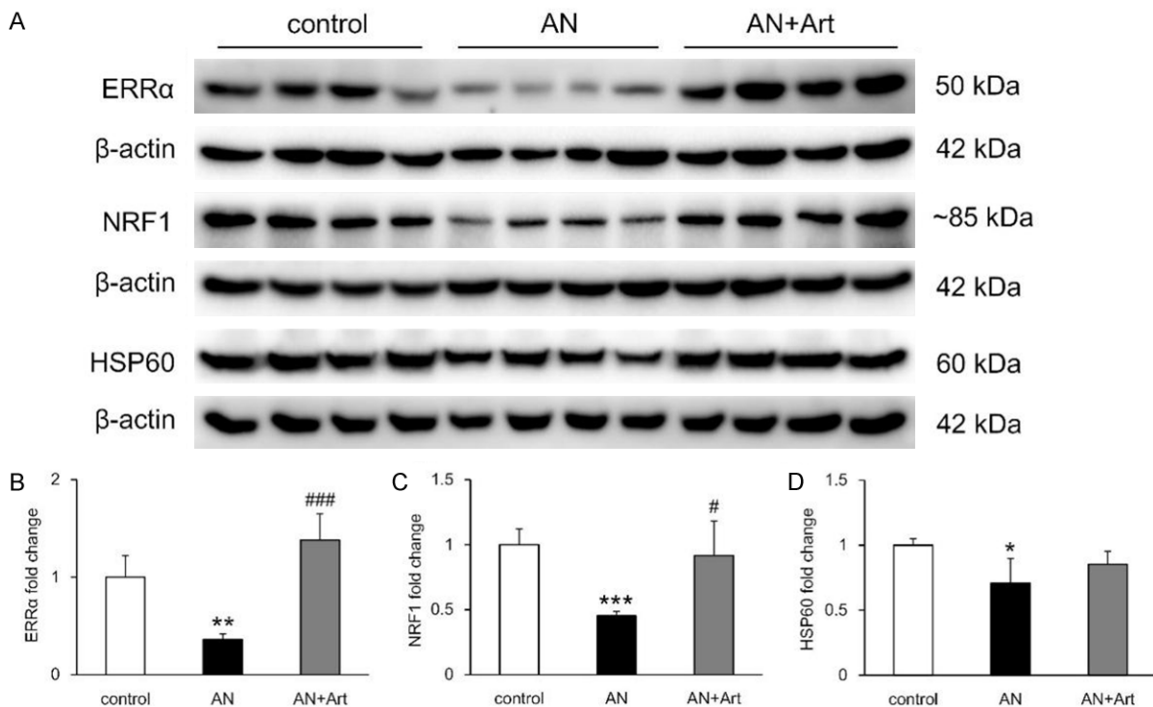


**Figure 7.** Artemether upregulated mitochondrial biogenesis related transcription factors. A. Immunoblotting bands of ERR $\alpha$ , NRF1, and HSP60 in various groups. B-D. Bar graphs showed the fold change of ERR $\alpha$ , NRF1, and HSP60 in each group. n=4 per group. \*P<0.05, \*\*P<0.01 and \*\*\*P<0.001 vs. control; #P<0.05 and ###P<0.001 vs. AN.

tional Chinese Medicine Hospital, The Fourth Clinical Medical College of Guangzhou University of Chinese Medicine, 1 Fuhua Road, Futian 518033, Shenzhen, Guangdong, China. E-mail: hanpengxin@126.com (PXH); sunhuili2011@126.com (HLS)

## References

- [1] Kalantar-Zadeh K, Jafar TH, Nitsch D, Neuen BL and Perkovic V. Chronic kidney disease. *Lancet* 2021; 398: 786-802.
- [2] Qi R and Yang C. Renal tubular epithelial cells: the neglected mediator of tubulointerstitial fibrosis after injury. *Cell Death Dis* 2018; 9: 1126.
- [3] Lee VW and Harris DC. Adriamycin nephropathy: a model of focal segmental glomerulosclerosis. *Nephrology (Carlton)* 2011; 16: 30-38.
- [4] Tan RJ, Li Y, Rush BM, Cerqueira DM, Zhou D, Fu H, Ho J, Beer Stolz D and Liu Y. Tubular injury triggers podocyte dysfunction by beta-catenin-driven release of MMP-7. *JCI Insight* 2019; 4: e122399.
- [5] Lovisa S, Zeisberg M and Kalluri R. Partial epithelial-to-mesenchymal transition and other new mechanisms of kidney fibrosis. *Trends Endocrinol Metab* 2016; 27: 681-695.
- [6] Jiang M, Bai M, Lei J, Xie Y, Xu S, Jia Z and Zhang A. Mitochondrial dysfunction and the AKI-to-CKD transition. *Am J Physiol Renal Physiol* 2020; 319: F1105-F1116.
- [7] Maekawa H and Inagi R. Pathophysiological role of organelle stress/crosstalk in AKI-to-CKD transition. *Semin Nephrol* 2019; 39: 581-588.
- [8] Wallace KB, Sardao VA and Oliveira PJ. Mitochondrial determinants of doxorubicin-induced cardiomyopathy. *Circ Res* 2020; 126: 926-941.
- [9] Prasanna PL, Renu K and Valsala Gopalakrishnan A. New molecular and biochemical insights of doxorubicin-induced hepatotoxicity. *Life Sci* 2020; 250: 117599.
- [10] Han P, Yuan C, Wang Y, Wang M, Weng W, Zhan H, Yu X, Wang T, Li Y, Shao M, Li S, Yi T and Sun H. Niclosamide ethanolamine protects kidney in adriamycin nephropathy by regulating mitochondrial redox balance. *Am J Transl Res* 2019; 11: 855-864.
- [11] Sheng L and Zhuang S. New insights into the role and mechanism of partial epithelial-mesenchymal transition in kidney fibrosis. *Front Physiol* 2020; 11: 569322.
- [12] Ma N, Zhang Z, Liao F, Jiang T and Tu Y. The birth of artemisinin. *Pharmacol Ther* 2020; 216: 107658.
- [13] Han P, Wang Y, Zhan H, Weng W, Yu X, Ge N, Wang W, Song G, Yi T, Li S, Shao M and Sun H. Artemether ameliorates type 2 diabetic kidney disease by increasing mitochondrial pyruvate carrier content in db/db mice. *Am J Transl Res* 2019; 11: 1389-1402.
- [14] Wang Y, Han P, Wang M, Weng W, Zhan H, Yu X, Yuan C, Shao M and Sun H. Artemether improves type 1 diabetic kidney disease by regulating mitochondrial function. *Am J Transl Res* 2019; 11: 3879-3889.
- [15] Han P, Cai Y, Wang Y, Weng W, Chen Y, Wang M, Zhan H, Yu X, Wang T, Shao M and Sun H. Artemether ameliorates kidney injury by restoring redox imbalance and improving mitochondrial function in Adriamycin nephropathy in mice. *Sci Rep* 2021; 11: 1266.
- [16] Bleicken S, Hofhaus G, Ugarte-Urbe B, Schroder R and Garcia-Saez AJ. cBid, Bax and Bcl-xL exhibit opposite membrane remodeling activities. *Cell Death Dis* 2016; 7: e2121.
- [17] Gray LR, Tompkins SC and Taylor EB. Regulation of pyruvate metabolism and human disease. *Cell Mol Life Sci* 2014; 71: 2577-2604.
- [18] Park S, Jeon JH, Min BK, Ha CM, Thoudam T, Park BY and Lee IK. Role of the pyruvate dehydrogenase complex in metabolic remodeling: differential pyruvate dehydrogenase complex functions in metabolism. *Diabetes Metab J* 2018; 42: 270-281.
- [19] Lee H and Yoon Y. Mitochondrial membrane dynamics-functional positioning of OPA1. *Antioxidants (Basel)* 2018; 7: 186.
- [20] Rosencrans WM, Rajendran M, Bezrukov SM and Rostovtseva TK. VDAC regulation of mitochondrial calcium flux: from channel biophysics to disease. *Cell Calcium* 2021; 94: 102356.
- [21] Sies H and Jones DP. Reactive oxygen species (ROS) as pleiotropic physiological signalling agents. *Nat Rev Mol Cell Biol* 2020; 21: 363-383.
- [22] Ix JH and Shlipak MG. The promise of tubule biomarkers in kidney disease: a review. *Am J Kidney Dis* 2021; 78: 719-727.
- [23] Denker BM and Sabath E. The biology of epithelial cell tight junctions in the kidney. *J Am Soc Nephrol* 2011; 22: 622-625.
- [24] Tan JX and Finkel T. Mitochondria as intracellular signaling platforms in health and disease. *J Cell Biol* 2020; 219: e202002179.

- [25] Garenne D, Renault TT and Manon S. Bax mitochondrial relocation is linked to its phosphorylation and its interaction with Bcl-xL. *Microb Cell* 2016; 3: 597-605.
- [26] Lennicke C and Cocheme HM. Redox metabolism: ROS as specific molecular regulators of cell signaling and function. *Mol Cell* 2021; 81: 3691-3707.
- [27] Singh BK, Sinha RA, Tripathi M, Mendoza A, Ohba K, Sy JAC, Xie SY, Zhou J, Ho JP, Chang CY, Wu Y, Giguere V, Bay BH, Vanacker JM, Ghosh S, Gauthier K, Hollenberg AN, McDonnell DP and Yen PM. Thyroid hormone receptor and ERRalpha coordinately regulate mitochondrial fission, mitophagy, biogenesis, and function. *Sci Signal* 2018; 11: eaam5855.
- [28] Popov LD. Mitochondrial biogenesis: an update. *J Cell Mol Med* 2020; 24: 4892-4899.
- [29] Caruso Bavisotto C, Alberti G, Vitale AM, Paladino L, Campanella C, Rappa F, Gorska M, Conway de Macario E, Cappello F, Macario AJL and Marino Gammazza A. Hsp60 post-translational modifications: functional and pathological consequences. *Front Mol Biosci* 2020; 7: 95.